

Tunneling Theory for Tunable Open Quantum Systems of Ultracold Atoms in One-Dimensional Traps

R. Lundmark,¹ C. Forssén,^{1,2,3,*} and J. Rotureau¹

¹*Department of Fundamental Physics, Chalmers University of Technology, SE-412 96 Göteborg, Sweden*

²*Department of Physics and Astronomy, University of Tennessee, Knoxville, TN 37996, USA*

³*Physics Division, Oak Ridge National Laboratory, Oak Ridge, TN 37831, USA*

The creation of tunable open quantum systems is becoming feasible in current experiments with ultracold atoms in low-dimensional traps. In particular, the high degree of experimental control over these systems allows detailed studies of tunneling dynamics, e.g., as a function of the trapping geometry and the interparticle interaction strength. In order to address this exciting opportunity we present a theoretical framework for two-body tunneling based on the rigged Hilbert space formulation. In this approach, bound, resonant and scattering states are included on an equal footing, and we argue that the coupling of all these components is vital for a correct description of the relevant threshold phenomena. In particular, we study the tunneling mechanism for two-body systems in one-dimensional traps and different interaction regimes. We find a strong dominance of sequential tunneling of single particles for repulsive and weakly attractive systems, while there is a signature of correlated pair tunneling in the calculated many-particle flux for strongly attractive interparticle interaction.

PACS numbers: 67.85.Lm, 03.75.Lm, 74.50.+r, 24.30.Gd

Introduction. The tunneling of particles, energetically confined by a potential barrier, is a fascinating quantum phenomenon which plays an important role in many physical systems. In nuclear physics, the tunneling process was first discussed in the context of alpha decay [1]. For multiparticle decay, the emission process gets more involved as the interaction between the emitted particles can strongly impact the decay probability. The relative importance of sequential (i.e., successive single-particle) and non-sequential decay channels is a pivotal question for such many-body systems, and the general phenomenon of pairing in fermionic systems [2–6] becomes very relevant. For example, the nuclear pairing interaction is known to enhance the probability of two-proton radioactivity [7–10]. Furthermore, the Coulomb interaction between electrons plays a crucial role in the double ionization of atoms [11, 12], although a full theoretical understanding of this two-body decay is still lacking.

An exciting recent development in the context of multiparticle tunneling is the experimental realization of few-body Fermi systems with ultracold atoms [13, 14]. These setups are extremely versatile as they are associated with a high degree of experimental control over key parameters such as the number of particles and the shape of the confining potential. In addition, the interaction between particles can be tuned using Feshbach resonances [15], which in the case of trapped particles turns into a confinement-induced resonance [16, 17]. The resulting interparticle interaction is of very short range compared to the size of the systems, and can be modeled with high accuracy by a zero-range potential. Such tunable open quantum systems provides a unique opportunity to investigate the

mechanism of tunneling as a function of the trap geometry and the strength of the interparticle interaction.

The dynamics of quantum tunneling can be naturally modeled using time-dependent theoretical approaches. See for example Refs. [18–21] for studies of two-atom tunneling with repulsive interactions and idealized geometries, and Refs. [10, 22] for attractive interactions. Different dynamical regimes of multiparticle tunneling through a thin barrier was discussed in Refs. [23–25] with a focus on the effects of quantum statistics. In addition, the single-particle and pair tunneling of trapped fermionic atoms with attractive interactions were recently studied employing a time-independent quasiparticle formalism [26, 27] in which the tunneling rate was obtained using the semiclassical Wentzel-Kramers-Brillouin (WKB) approximation. However, that approach suffers from the uncontrolled approximation of artificially dividing the space into different regions. The time-dependent approaches, on the other hand, are not very reliable when the decay width is small and they are not easily extended to many-particle systems.

The purpose of this Rapid Communication is to introduce an alternative approach to the study of open quantum systems with ultracold atoms. Our method is based on the rigged Hilbert space formulation, that extends beyond the domain of hermitian quantum mechanics and includes also time-asymmetric processes such as decays (see e.g. Ref. [28] and references therein). In nuclear physics this formulation has been employed in the Gamow Shell Model [29–34] to study threshold states and decay processes. Recently, it has also been used to model near-threshold, bound states of dipolar molecules [35]. Here, we focus on the basic example of two interacting atoms in a one-dimensional (1D) trap, and we present results that highlight the importance of a unified treatment of bound, resonant and scattering states for the proper

* christian.forssen@chalmers.se

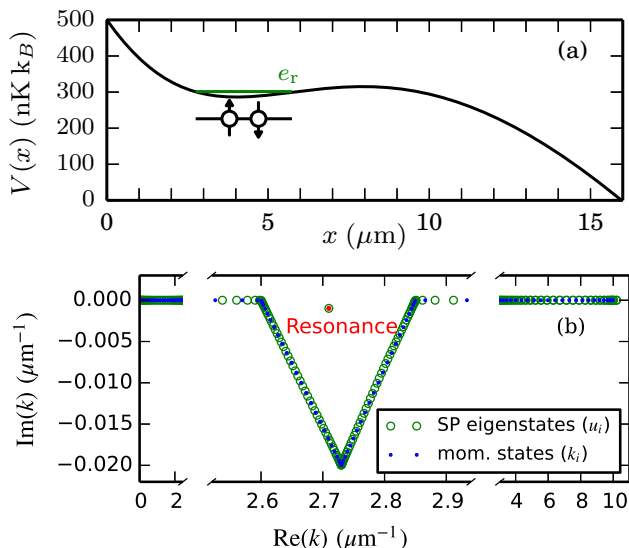


FIG. 1. (Color online) Panel (a): Trap potential, indicating the position of SP and two-body resonance states. Panel (b): Complex-momentum contour and Berggren basis states, highlighting the position of the SP resonance pole.

description of tunneling phenomena in ultracold atoms. We study in particular the decay mechanism, and we perform realistic calculations to make comparisons with recent experimental data [14].

Theoretical Formalism. We consider a system of interacting, two-component fermions in a finite-depth potential trap. The trap does not support any single-particle (SP) bound states, but is just deep enough to support a SP quasi-bound state with a finite lifetime. For definiteness, we employ a 1D potential corresponding to the experimental setup in Ref. [14], as illustrated in Fig. 1(a). Let us denote this potential $V(x)$, with x the degree of freedom in the direction of the trap. The interaction between fermionic atoms in different hyperfine states is modeled by the zero-range potential $V^\delta(x, x') = g\delta(x - x')$, with g the tunable interaction strength. The fermions will be referred according to their hyperfine spin state as “spin-up” (\uparrow) and “spin-down” (\downarrow), thus making an obvious connection with systems of spin 1/2 particles (e.g. electrons or nucleons). In this Rapid Communication we will restrict ourselves to the simplest instance of such a tunable open quantum system, the case of two interacting fermions in different spin states in an open 1D potential trap. However, we want to stress that the formalism can be applied to higher-dimensional traps and to systems with more particles.

The Hamiltonian for the two-particle system is

$$H = \sum_{i=1}^2 \left[-\frac{\hbar^2}{2m} \frac{d^2}{dx_i^2} + V(x_i) \right] + g\delta(x_1 - x_2), \quad (1)$$

with m the mass of the particle. Let us first consider the situation of two non-interacting particles, i.e., $g = 0$.

In this case, the ground state of the system, $|\Phi^{(0)}\rangle$, corresponds to the two distinguishable fermions both occupying the resonant (quasi-bound) state $|u_{\text{res}}\rangle$ of the SP Hamiltonian: $h(x) = -\hbar^2/(2m)d^2/dx^2 + V(x)$. In this configuration, both particles are localized in the trap for a finite amount of time, before tunneling out through the potential barrier. The decaying SP state $|u_{\text{res}}\rangle$ can be described as a Gamow state [1]. Such a state behaves asymptotically as an outgoing wave with a complex energy $e = e_r - i\gamma_r/2$. The imaginary part of the energy corresponds to the decay width γ_r and gives the half-life of the SP state, $t_{1/2} = \ln(2)\hbar/\gamma_r$, and the SP tunneling rate $\gamma_1 = \gamma_r/\hbar$.

We will obtain solutions of the two-body Hamiltonian (1), for finite values of the interaction strength g using an expansion of SP states in the so-called Berggren basis [36]. This complex-momentum basis includes S-matrix poles (bound and resonant states) as well as non-resonant scattering states associated with the potential $V(x)$. The use of this basis is key to our approach as it allows to consistently include the continuum when finding eigensolutions of the open quantum system. It constitutes a rigged Hilbert space and the corresponding completeness relation is a generalization of the Newton completeness relation [37] (defined only for real energy states) and reads

$$\sum_n |u_n\rangle \langle \tilde{u}_n| + \int_{L^+} dk |u_k\rangle \langle \tilde{u}_k| = 1, \quad (2)$$

where $|u_n\rangle$ correspond to poles of the S-matrix, and the integral of states along the contour L^+ , extending below the resonance poles in the fourth quadrant of the complex-momentum plane, represents the contribution from the non-resonant scattering continuum [36]. In practice, the integral in (2) is discretized in two steps. First, the contour L^+ is truncated at $k = k_{\text{max}}$ and each segment is spanned by a Gauss-Legendre mesh that gives a finite set of complex-momentum states $\{|k_i\rangle\}$. In a second step, the SP Hamiltonian is diagonalized in order to obtain a finite set of SP basis states $U_1 \equiv \{|u_i\rangle\}$ [32]. The two-particle basis T_2 is then naturally constructed from the SP basis for the spin-up and -down fermions as $T_2 \equiv U_1(\uparrow) \otimes U_1(\downarrow)$. For the SP states along the complex contour, the wave function diverges for $x \rightarrow \infty$ and as a consequence, the matrix elements of the two-body interaction in the Berggren basis are not finite. We solve this issue by regularizing the two-body matrix elements between states in T_2 using an expansion in the harmonic oscillator (HO) basis [31]. Note that our Hamiltonian (1) matrix in this rigged Hilbert space will be non-Hermitian, but complex symmetric. The spectrum will include bound, resonant and scattering many-body states. Resonance solutions, $|\Phi_{\text{res}}\rangle$, are characterized by outgoing boundary conditions and a complex energy $E = E_r - i\Gamma_r/2$, where Γ_r is the decay width due to the emission of particles out of the trap. The resonant solution will be identified in the many-body spectrum, as the state with the largest overlap (in modulus) with

$|\Phi^{(0)}\rangle$, referred to as the pole approximation [29]. With this goal in mind we employ the Davidson algorithm for diagonalization [38, 39] which allows to target a desired eigenpair. Note that results for low-energy resonances should be independent of the particular choice of L^+ as long as the Berggren completeness relation (2) holds, i.e., k_{\max} and the number of discretization points both need to be large enough.

Concerning the tunneling rate we want to stress that there is *a priori* no simple relation between the decay width and the half life for a many-body system, contrary to the case of a SP Gamow state. Assuming exponential decay we would estimate the tunneling rate $\gamma_{\Gamma} = \Gamma_r/\hbar = -2\text{Im}(E)/\hbar$. However, having access to the resonant wave function, $\Phi_{\text{res}}(x_1, x_2) \equiv \Phi_{\text{res}}(\mathbf{x})$, we can alternatively compute the decay rate using an integral formalism [9]. The rate of particle emissions can be obtained by integrating the outward flux of particles at large distance x_{out} from the center of the trap, and normalizing by the number of particles on the inside

$$\gamma_{\text{flux}} = \frac{\hbar}{imN(x_{\text{out}})} \sum_i \int_0^{x_{\text{out}}} \prod_{j \neq i} dx_j \left[\Phi_{\text{res}}^*(\mathbf{x}) \frac{d}{dx_i} \Phi_{\text{res}}(\mathbf{x}) - \left(\frac{d}{dx_i} \Phi_{\text{res}}^*(\mathbf{x}) \right) \Phi_{\text{res}}(\mathbf{x}) \right]_{x_i=x_{\text{out}}}, \quad (3)$$

with $N(x_{\text{out}}) = \int_0^{x_{\text{out}}} \prod_j dx_j |\Phi_{\text{res}}(\mathbf{x})|^2$.

Results. In the experimental setup of Ref. [14], the fermions are trapped in an effective 1D optical trap created by a tightly focused laser beam (Rayleigh range x_R) combined with a linear magnetic potential (magnetic field gradient B') giving the potential

$$V(x) = pV_0 \left(1 - \frac{1}{1 + \left(\frac{x}{x_R}\right)^2} \right) - c_{B,\sigma} \mu_B B' x. \quad (4)$$

The depth pV_0 of the trapping potential depends on the number of particles that are in the trap. In addition, the parameter $c_{B,\sigma} \approx 1$, although the exact value depends on both the magnetic-field strength and the spin of the particle. For comparison with experimental results we will use molecular units, in which energy is given in nK k_B , time in μs , and distances in μm . In these units we have $\hbar = 7638.2 \text{ nK } k_B \mu\text{s}$, the Bohr magneton $\mu_B = 6.7171 \cdot 10^8 \text{ nK } k_B \text{ T}^{-1}$ and $\hbar^2/m = 80.645 \text{ nK } k_B \mu\text{m}^2$, where m is the mass of a ${}^6\text{Li}$ atom.

In Fig. 1(a) we show for illustrative purpose the trap potential with $pV_0 = 2.123 \cdot 10^3 \text{ nK } k_B$, $x_R = 9.975 \mu\text{m}$, $B' = 18.90 \cdot 10^{-8} \text{ T } \mu\text{m}^{-1}$, $c_{B,\sigma} = 1$ which closely resemble the parameters extracted from experimental data (see also discussion below). In order to handle the linear term $B'x$ we truncate the potential at x_{cut} , sufficiently far away from the relevant trap region. In practice, this is achieved by applying a positive energy shift E_{shift} so that $V(x_{\text{cut}}) + E_{\text{shift}} = 0$. The energy shift is subtracted

at the end, and we have verified that the fluctuations in the SP energy (tunneling rate) with the choice of E_{shift} was less than 0.04% (2%).

The SP Schrödinger equation is solved using the method described above. The discrete set of complex-momentum states $\{|k_i\rangle\}$ that span the contour L^+ is shown as blue dots in Fig. 1(b). The energy shift that was used is $E_{\text{shift}} = 500 \text{ nK } k_B$. The resulting set of eigenstates (green circles) lies very close to the contour with the exception of one isolated state. The former states correspond to non-resonant scattering solutions, while the latter is a resonance. Together, these eigenstates form the complete set of SP basis states, $\{|u_i\rangle\}$, that will be used in the many-body calculation.

The number of points on the contour is increased until convergence of the SP resonance energy is achieved. Note that the resonance pole will always remain fixed while the set of scattering states will depend on the choice of the contour L^+ . For illustration purposes, the contour shown in Fig. 1 consists of only $N_{\text{pts}} = 100$ basis states while full calculations were performed with $N_{\text{pts}} = 240\text{--}320$. For this set of potential parameters we find $e = (301.415 - 0.085i) \text{ nK } k_B$, which translates into a tunneling rate $\gamma_1 = 22.38 \text{ s}^{-1}$.

We now consider the solution of the interacting two-fermion system, projected on the full Berggren basis. We define the interaction energy as

$$E_{\text{int}} \equiv \text{Re}(E) - 2e_r, \quad (5)$$

where $\text{Re}(E) = E_r$ is the real part of the resonance energy. Results for the two-particle resonance state as a function of the interaction strength g are shown in Fig. 2. For $g = 0$, the two fermions tunnel out independently and the tunneling rate is equal to $\gamma = 2\gamma_1 = 44.76 \text{ s}^{-1}$. However, as the interaction becomes more attractive, the real part of the resonance energy decreases, and the effective barrier seen by the two particles increases. As a consequence the tunneling rate decreases as seen in Fig. 2(b).

Along with the full calculations, we show in Fig. 2 also results obtained in the pole approximation, which corresponds to the single configuration where the two distinguishable fermions occupy the SP resonant state. This comparison clearly demonstrates the importance of continuum correlations. The resonance energy and width are both decreased due to configuration mixing between the SP resonance pole and non-resonant scattering states. In particular, the energy width, which translates into a decay rate, is very sensitive to these correlations. These results highlight the importance of properly taking the openness of the system into account.

The agreement between the tunneling rate computed from the decay width of the resonance and from the flux formula (3) demonstrates the quality of our numerical approach. It also shows that the tunneling is well approximated by an exponential decay law for this system. The numerical precision of results obtained in our approach was studied in a series of convergence studies for systems with different interaction strengths

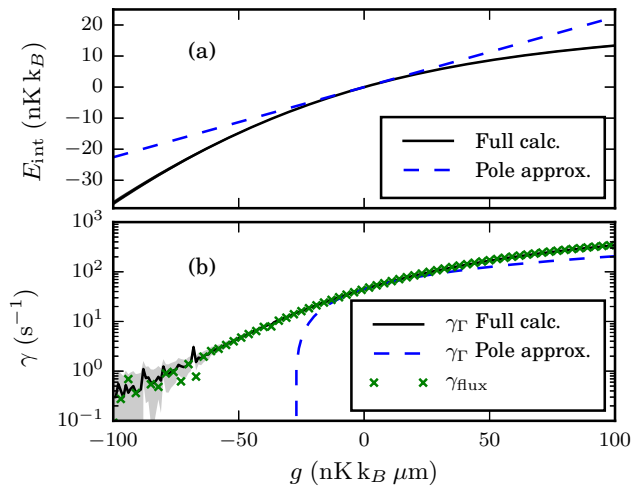


FIG. 2. (Color online) Two-fermion resonance state as a function of the interaction strength g for $c_B = 1$. Panel (a): Interaction energy (5) compared with the corresponding energy obtained using the pole approximation. Panel (b): Tunneling rates obtained from the imaginary part of the resonance energy (from the full calculation and the pole approximation, respectively) compared with the rate obtained from the flux calculation (3).

($g = +100, -20, -100$ nK $k_B \mu\text{m}$). We varied the number of discretization points, modified the contour in the complex-momentum plane, or changed the number of HO states in the computation of interaction matrix elements (for a detailed discussion of these studies, see Ref. [40]). An uncertainty on the numerical results for a specific coupling coefficient was then extracted based on the amplitudes of variations when these model-space parameters were varied one by one. Adding these amplitudes in quadrature gave an uncertainty in the real part of the interaction energy on the order of $\lesssim 2\%$ for the entire range of interaction strengths. However, the precision of the computed imaginary energy was found to have a lower bound since variations of the computed decay rate was never smaller than 0.5 s^{-1} . This becomes obvious when the interaction is strongly attractive and the ratio of imaginary and real energies turns out to be very small. On the other hand, for larger decay rates the variations were on the order of $\lesssim 1\%$. In combination we have $\Delta\gamma = \max(0.01\gamma, 0.5 \text{ s}^{-1})$. This observation can be qualitatively understood in the following way: The precision of the computed (complex) energy is not strongly dependent on the value of g . For the most repulsive interactions, the values of the real and imaginary parts are much larger than this precision. However, as the interaction becomes more attractive, the imaginary part rapidly decreases. With the precision of the total (complex) energy almost constant, this creates a much larger (relative) uncertainty for the tunneling rate in this region. The estimated uncertainties from these numerical studies are shown as shaded bands in both panels of Fig. 2, but is

only visible in the tunneling rate for the most attractive interactions ($g \lesssim -60$ nK $k_B \mu\text{m}$).

Density and Tunneling Mechanism. The density and stationary outgoing particle flux can be seen in Fig. 3 for attractive and repulsive interactions. The particles are localized around the trap minimum (at approximately $x = 4 \mu\text{m}$). For the repulsive interaction shown in Fig. 3(a) we can clearly observe the emerging fermionization [41–43] of the two distinguishable particles by the development of an $x_1 = x_2$ valley in the density distribution.

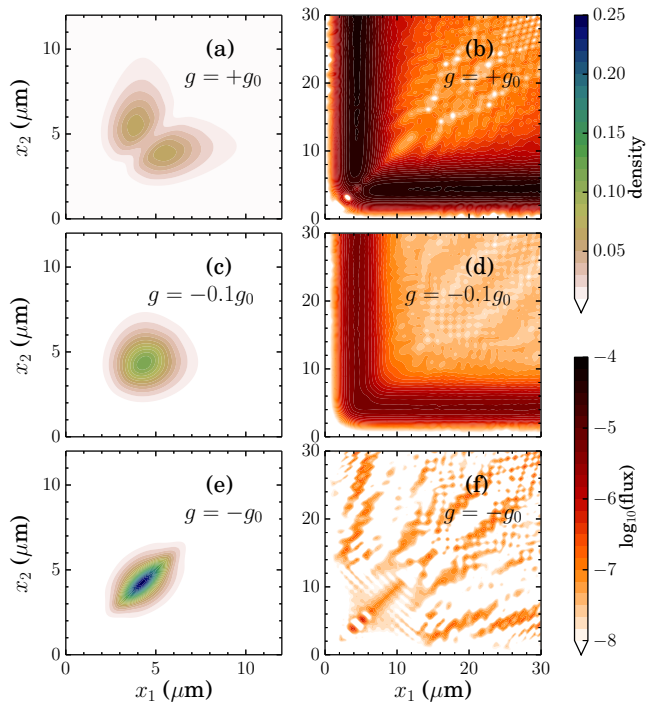


FIG. 3. (Color online) Density contour plots (left panels) and logarithm of the outward particle flux (right panels) for repulsive ($g = +g_0$), slightly attractive ($g = -0.1g_0$), and strongly attractive ($g = -g_0$) interactions (with $g_0 = 100$ nK $k_B \mu\text{m}$) from top to bottom, respectively.

The flux provides interesting insights into the tunneling mechanism. For the repulsive and the slightly attractive scenarios, shown in Figs. 3(b,d), the outgoing flux is mainly concentrated in two bands, corresponding to one particle staying in the trap and the other one leaving it. This indicates a strong predominance of sequential tunneling. However, for the most attractive case, shown in Fig. 3(f), we have significant outward flux in the $x_1 \approx x_2$ region. This signals that the two fermions can leave the trap simultaneously at short distance from each other. Unfortunately, the region of strong attraction, where pair tunneling appears as an important decay channel, is also characterized by the smallest total tunneling rates. Therefore, there is significant numerical noise for these particular results. We stress, however, that the general conclusion of increasing pair tunneling

remains true although quantitative results cannot be obtained.

Comparison with Experimental Data. The tunneling of few fermions from low-dimensional traps were measured by Zürn et al. [14]. The experimental trap was highly elongated with a much stronger confinement in the perpendicular direction, $\omega_{\parallel}/\omega_{\perp} \approx 1/10$. Still, for very strong attraction the size of the dimer can become comparable to b_{\perp} , the length scale of the ignored (transverse) trap dimensions. In such a situation, the 1D approximation could be questioned. Following Ref. [42] we have verified that we remain in the effectively one-dimensional region with $a_{1D}/b_{\perp} \approx 3$ for $g = -100 \text{ nK k}_B \mu\text{m}$, which is the largest attraction considered in this Rapid Communication.

The data analysis of Ref. [14] is quite complicated and involves the use of the WKB approximation to extract the trap potential parameters. More precisely, pV_0 and B' in Eq. (4) were adjusted such that the SP tunneling rates obtained in the WKB approximation matched the experimental results. Using the set of parameters given in Ref. [14] as input to our exact diagonalization approach leads to good agreement for the SP energies (with a difference of at most a few percent), while SP tunneling rates were almost two times larger than the ones published in Ref. [14]. As a consequence, we have adopted the strategy of refitting the parameters p and B' to reproduce measured SP tunneling rates. Resulting changes of these parameters, compared to the WKB analysis, is in the order of $\sim 0.1\%$. From this one can conclude that the tunneling rate is very sensitive to small shifts in the trapping potential, that continuum couplings are very important, and that the uncontrolled WKB approximation may be inadequate to use in a fitting procedure.

Using this new set of parameters, we compute the energies and the tunneling rates for the two-particle system. For these calculations we used a complex-momentum contour with slightly fewer discretization points ($N_{\text{pts}} = 200$). Our predictions are presented in Table I compared to experimental data. The calculated tunneling rates are

g (nK k _B μm)	E_{int} (nK k _B)	γ_{Γ} (s ⁻¹)	γ_{Exp} (s ⁻¹)
-31.0	-8.4(2)	19.2(5)	22.2(10)
-41.5	-12.1(3)	12.5(5)	13.8(10)
-45.0	-13.6(3)	25.8(5)	9.7(3)
-99.9	-37.0(7)	0.4(5)	2.14(20)

TABLE I. Energy and tunneling rate for two atoms in a trap as a function of the interaction strength g . Experimental results from Zürn et al. [14]. Each case corresponds to a different trapping potential, as described in the text.

in acceptable agreement with the measured ones. However, for one case ($g = -45.0 \text{ nK k}_B \mu\text{m}$) the difference is almost a factor three, which is well beyond the expected precision of our method as indicated by the uncertainty estimates of the tabulated results. The fact that our tunneling rate is not monotonically decreasing

as the interaction becomes more attractive is due to the extreme dependence on the SP potential. In particular, for each value of g , the parameter $c_{B,\sigma}$ is slightly different. Moreover, the spin dependence of this term gives rise to slightly different trapping potentials for the two atoms. Unfortunately, this parameter is not determined uniquely by the SP tunneling data and we have therefore used $c_{B,\sigma}(g)$ as published in Ref. [14]. A better agreement with the experimental results can certainly be achieved by relaxing the predictive ambitions and tuning this parameter for each specific interaction strength. As a final note, our calculated interaction energies are about three times larger than the values extracted (using WKB) from experiment. We conclude that the WKB method should not be expected to produce reliable estimates for this quantity and that the analysis of experimental results for open quantum systems is highly sensitive to the determination of trap parameters.

Conclusion. In this Rapid Communication we have introduced the rigged Hilbert space formalism to the theoretical study of tunneling in systems of ultracold atoms. We focused on the case of two distinguishable particles in a one-dimensional trap. The two-atom dynamics was solved for a wide range of interaction strengths by using an expansion in the Berggren basis. The computational cost of this approach is mainly associated with the construction of the Hamiltonian matrix. Fortunately, the two-body interaction matrix elements are directly proportional to the interaction strength g and will only have to be computed once for a specific model-space truncation. We computed the energy and lifetime of two-body resonant states, and could highlight the importance of continuum correlations for the proper description of such threshold phenomena. Moreover, we were able to obtain the density and flux distributions. The analysis of the outgoing particle flux indicated a predominance of sequential single-particle tunneling, with signs of pair tunneling for strongly attractive systems. The numerical robustness of our method was discussed and our theoretical predictions were compared with experimental results. We found a quantitative agreement for tunneling rates in systems with attractive interactions. However, interaction energies differed significantly from those extracted from experimental data using a WKB approach [14] and we emphasized that these differences stem from the uncontrolled approximation inherent to semiclassical approaches.

Our approach offers a number of key features: As we use an expansion in a SP basis, the particle statistics of the many-body states is treated exactly and the method can be straightforwardly extended to systems with more atoms and other shapes for the trapping potential. By working in a rigged Hilbert space we actually compute the complex energies of true many-body resonances, which gives us both the position and the width. The numerical precision of the method will be limited by the relative magnitude of real and imaginary energies. Still, the two-body systems that are studied in this work

range from strongly repulsive to strongly attractive, and the associated decay rates span three orders of magnitude.

Acknowledgments. The research leading to these results has received funding from the European Research Council under the European Community's Seventh Framework Programme (FP7/2007-2013) / ERC grant agreement no. 240603, and the Swedish Foundation for International Cooperation in Research and Higher Education (STINT, IG2012-5158). The computations

were performed on resources provided by the Swedish National Infrastructure for Computing (SNIC) at High-Performance Computing Center North (HPC2N) and at Chalmers Centre for Computational Science and Engineering (C3SE). We thank the European Centre for Theoretical Studies in Nuclear physics and Related Areas (ECT*) in Trento, and the Institute for Nuclear Theory at the University of Washington, for their hospitality and partial support during the completion of this work. We are much indebted to D. Blume, M. Zhukov, N. Zinner, and G. Zürn for stimulating discussions.

-
- [1] G. Gamow, *Zeitschrift für Physik* **51**, 204 (1928).
- [2] P. De Gennes, *Superconductivity Of Metals And Alloys*, Advanced Books Classics Series (Westview Press, 1999), ISBN 9780813345840.
- [3] J. Bardeen, L. N. Cooper, and J. R. Schrieffer, *Phys. Rev. Lett.* **108**, 1175 (1957).
- [4] A. B. Migdal, *Nucl. Phys.* **13**, 655 (1959).
- [5] A. Bohr and B. Mottelson, *Nuclear Structure*, Vol. I and II (World Scientific, 1998), ISBN 9789810239794.
- [6] G. Baym, C. Pethick, and D. Pines, *Nature* **224**, 673 (1969).
- [7] M. Pfützner, M. Karny, L. V. Grigorenko, and K. Riisager, *Rev. Mod. Phys.* **84**, 567 (2012).
- [8] L. V. Grigorenko, R. C. Johnson, I. G. Mukha, I. J. Thompson, and M. V. Zhukov, *Phys. Rev. Lett.* **85**, 22 (2000).
- [9] L. V. Grigorenko and M. V. Zhukov, *Phys. Rev. C* **76**, 014008 (2007).
- [10] T. Maruyama, T. Oishi, K. Hagino, and H. Sagawa, *Phys. Rev. C* **86**, 044301 (2012).
- [11] A. N. Pfeiffer, C. Cirelli, M. Smolarski, R. Dörner, and U. Keller, *Nat Phys* **7**, 428 (2011).
- [12] B. Walker, B. Sheehy, L. F. DiMauro, P. Agostini, K. J. Schafer, and K. C. Kulander, *Phys. Rev. Lett.* **73**, 1227 (1994).
- [13] F. Serwane, G. Zürn, T. Lompe, T. B. Ottenstein, A. N. Wenz, and S. Jochim, *Science* **332**, 336 (2011).
- [14] G. Zürn, A. N. Wenz, S. Murmann, A. Bergschneider, T. Lompe, and S. Jochim, *Phys. Rev. Lett.* **111**, 175302 (2013).
- [15] C. Chin, R. Grimm, P. Julienne, and E. Tiesinga, *Rev. Mod. Phys.* **82**, 1225 (2010).
- [16] M. Olshanii, *Phys. Rev. Lett.* **81**, 938 (1998).
- [17] G. Zürn, T. Lompe, A. N. Wenz, S. Jochim, P. S. Julienne, and J. M. Hutson, *Phys. Rev. Lett.* **110**, 135301 (2013).
- [18] A. U. J. Lode, A. I. Streltsov, O. E. Alon, H.-D. Meyer, and L. S. Cederbaum, *J. Phys. B* **42**, 044018 (2009).
- [19] S. Kim and J. Brand, *J. Phys. B* **44**, 195301 (2011).
- [20] A. U. J. Lode, A. I. Streltsov, K. Sakmann, O. E. Alon, and L. S. Cederbaum, *PNAS* **109**, 13521 (2012).
- [21] S. Hunn, K. Zimmermann, M. Hiller, and A. Buchleitner, *Phys. Rev. A* **87**, 043626 (2013).
- [22] T. Taniguchi and S. I. Sawada, *Phys. Rev. E* **83**, 026208 (2011).
- [23] A. del Campo, F. Delgado, G. García-Calderón, J. Muga, and M. Raizen, *Phys. Rev. A* **74**, 013605 (2006).
- [24] A. del Campo, *Phys. Rev. A* **84**, 012113 (2011).
- [25] M. Pons, D. Sokolovski, and A. del Campo, *Phys. Rev. A* **85**, 022107 (2012).
- [26] M. Rontani, *Phys. Rev. Lett.* **108**, 115302 (2012).
- [27] M. Rontani, *Phys. Rev. A* **88**, 043633 (2013).
- [28] R. de la Madrid, *Eur. J. Phys.* **26**, 287 (2005).
- [29] N. Michel, W. Nazarewicz, M. Płoszajczak, and K. Benceur, *Phys. Rev. Lett.* **89**, 042502 (2002).
- [30] J. Rotureau, N. Michel, W. Nazarewicz, M. Płoszajczak, and J. Dukelsky, *Phys. Rev. Lett.* **97**, 110603 (2006).
- [31] G. Hagen, M. Hjorth-Jensen, and N. Michel, *Phys. Rev. C* **73**, 064307 (2006).
- [32] N. Michel, W. Nazarewicz, M. Płoszajczak, and T. Vertse, *J. Phys. G* **36**, 013101 (2009).
- [33] G. Papadimitriou, A. T. Kruppa, N. Michel, W. Nazarewicz, M. Płoszajczak, and J. Rotureau, *Phys. Rev. C* **84**, 051304 (2011).
- [34] J. Rotureau and U. van Kolck, *Few-Body Syst* **54**, 725 (2013).
- [35] K. Fosseuz, N. Michel, W. Nazarewicz, and M. Płoszajczak, *Phys. Rev. A* **87**, 042515 (2013).
- [36] T. Berggren, *Nucl. Phys.* **A109**, 265 (1968).
- [37] R. G. Newton, *J. Math. Phys.* **1**, 319 (1960).
- [38] E. R. Davidson, *J. Comput. Phys.* **17**, 87 (1975).
- [39] N. Michel, W. Nazarewicz, M. Płoszajczak, and J. Okolowicz, *Phys. Rev. C* **67** (2003).
- [40] C. Forssén, R. Lundmark, and J. Rotureau (2014), in Proceedings of "Dynamics of Critically Stable Quantum Few-Body Systems (Critical Stability 2014)", edited by T. Frederico (in preparation).
- [41] M. Girardeau, *J. Math. Phys.* **1**, 516 (1960).
- [42] S. E. Gharashi and D. Blume, *Phys. Rev. Lett.* **111**, 045302 (2013).
- [43] E. J. Lindgren, J. Rotureau, C. Forssén, A. G. Volosniev, and N. T. Zinner, *New J. Phys.* **16**, 063003 (2014).